Increase in flood risk resulting from climate change in a developed urban watershed– The role of storm temporal patterns

Suresh Hettiarachchi[1], Conrad Wasko[1], and Ashish Sharma[1*]

[1]School of Civil and Environmental Engineering, University of New South Wales, Sydney, Australia.

*Corresponding author, Prof. Ashish Sharma, A.Sharma@unsw.edu.au

Abstract

Effects of climate change are causing more frequent extreme rainfall events and an increased risk of flooding in developed areas. Quantifying this increased risk is of critical importance for the protection of life and property as well as for infrastructure planning and design. The updated NOAA Atlas 14 intensity-duration-frequency (IDF) relationships and temporal patterns are widely used in hydrologic and hydraulic modelling for design and planning in the USA. Current literature shows that a rising temperatures as a result of climate change will result in an intensification of rainfall. These impacts are not explicitly included in the NOAA temporal patterns , which can have consequences on the design and planning of adaptation and flood mitigation measures. In addition there is a lack of detailed hydraulics modelling when assessing climate change impacts on flooding. The study presented in this manuscript uses a comprehensive hydrologic and hydraulic model of a fully developed urban/suburban catchment to explore two primary questions related to climate change impacts on flood risk: (1) How do climate change effects on storm temporal patterns and rainfall volumes impact flooding in a developed complex watershed? (2) Is the storm temporal pattern as critical as the total volume of rainfall when evaluating urban flood risk? We use the NOAA Atlas 14 temporal patterns along with the expected increase in temperature for the RCP8.5 scenario for 2081-2100, to project temporal patterns and rainfall volumes to reflect future climatic change. The model results show that different rainfall patterns cause variability in flood depths during a storm event. The changes in the projected temporal patterns alone increase the risk of flood magnitude upto 35 % with the cumulative impacts of temperature rise on temporal pattern and the storm volume increasing flood risk from 10 to 170 %. The results also show that regional storage facilities are sensitive to rainfall patterns that are loaded at the latter part of the storm duration while extremely intense short duration storms will cause flooding at all locations. This study shows that changes in temporal patterns will have a significant impact

on urban/suburban flooding and need to be carefully considered and adjusted to account for climate change when used for design and planning future stormwater systems.

1 Introduction

Recent history shows that extreme weather events are occurring more frequently and in areas that have not had such events in the past (Hartmann et al., 2013). There are more land regions where the number of heavy rainfall events has increased compared to where they have decreased (Alexander et al., 2006; Donat et al., 2013; Westra et al., 2013a). Intensification of rainfall extremes (Lenderink and van Meijgaard, 2008; Wasko and Sharma, 2015; Wasko et al., 2016b) and their increasing volume (Mishra et al., 2012; Trenberth, 2011) has been linked to the higher temperatures expected with climate change. This increase in the likelihood of extreme rainfall and its intensification creates a higher risk of damaging flood events that cause a threat to both life and the built environment, particular in urban regions where the existing infrastructure has not been designed to cope with these increases. Adapting to future extreme storm events (i.e. flood events) will be costly both economically and socially (Doocy et al., 2013). Properly addressing this increased flood risk is all the more important given the expectation that the urban population is projected to grow from the current 54 % to 66 % of the global population by the year 2050 (United Nations, 2014).

Adaptation as a way to address the effects of climate change has only recently gained attention (Mamo, 2015). Adaptation in the context of flood risk involves taking practical and proactive action to adjust or modify stormwater management infrastructure such as low impact development (LID) methods to reduce surface runoff or constructed storages to handle the increased flows during an extreme storm. The foundation of adaptation measures to deal with flooding is typically based on flood forecasting and hydrologic/hydraulic (H/H) modelling (Thodsen, 2007). The effectiveness of adaptation is dependent on the accuracy of simulating projected impacts, such as the effectiveness of a flood control structure to protect a city from future increased flooding. In addition, variability and uncertainty related to these flood forecasts play an important role since uncertainty in future projection limits the amount of adaptation that society will accept (Adger et al., 2009). Prior to the advent of computers and the increase in computational power, drainage design was based on simple empirical models of peak discharge rates using methods such as the rational formula in combination with Intensity-Duration-Frequency (IDF) curves (Adams and Howard, 1986; Nguyen et al.,

2010). Consideration of the environmental impacts related to flow rates, volumes, water quality and downstream impacts requires more complex systems and ways to simulate the hydrologic and hydraulic processes in a more realistic manner (Nguyen et al., 2010). As such, the state of the art in modelling urban sewer and stormwater related infrastructure uses distributed, fully dynamic, hydrologic and hydraulics modelling software (Singh and Woolhiser, 2002). The dynamic approach and integrated nature of current modelling requires the use of temporal patterns to distribute rainfall and volumes that closely resemble actual storm events (Nguyen et al., 2010; Rivard, 1996).

Temporal patterns have typically been derived using the alternating block method from IDF curves where shorter storm durations are nested within longer storm duration design intensities (García-Bartual and Andrés-Doménech, 2016; Victor Mockus and E. Woodward, 2015) . However, this method does not represent a real storm structure. Alternatively, Huff (1967) presented the first rigorous analysis of rainfall temporal patterns (García-Bartual and Andrés-Doménech, 2016), where rainfall temporal patterns were derived from observations. Similar methods include the average variability method, where a storm is partitioned into fractions of equal time, and each fraction is ranked. The temporal distribution is then specified as the most likely rainfall order with the average rainfall used for the associated fraction (Pilgrim, 1997). NOAA Atlas 14 provides an updated set of temporal distributions and IDF curves for use in a major portion of the United States (Perica, 2013) that are now widely used for planning and design modelling analysis. These temporal distributions and rainfall depths are based on observed data and were generated using methodology similar to Huff (1967). The major concern is that the analysis and methods used in Atlas 14 assumes a stationary climate over the period of observation and application (Chapter 4.5.4 of Atlas 14 volume 8). This seems contrary to prevailing scientific thought (Milly et al., 2007) and can lead to inadequacies of future stormwater infrastructure as there is evidence to believe that warmer temperatures are forcing intensification of temporal patterns (Wasko and Sharma, 2015) and an increase in variability (Mamo, 2015). Several previous studies have examined the sensitivity of urban catchments to changes in intensity and temporal patterns with peak runoff rates and volumes modelled (Lambourne and Stephenson, 1987; Mamo, 2015; Nguyen et al., 2010; Zhou et al., 2016). For example, Lambourne and Stephenson (1987) presented a comparative model study to look at the impact of temporal patterns on peak discharge rates and volumes. However, with the exception Zhou et al. (2016), these studies largely ignored the detailed hydraulic conveyance aspects of storage ponds, sewers, culverts, and flow

control structures which play an important role in how the flow rates generated during runoff move through and impact on the built environment.

Although there are an increasing number of catchment/basin scale and urban modelling studies that have been performed (Cameron, 2006; Graham et al., 2007; Leander et al., 2008; Zhou et al., 2016; Zope et al., 2016), there remains a lack of a detailed studies that looks at assessing future flood damage in a developed environment (Seneviratne et al., 2012). The majority of past studies focus on either the hydrologic modelling component or the rainfall intensity aspect and mostly overlook the crucial detail of rainfall patterns. In this study, we focus on the range of results generated from detailed H/H modelling arising from precipitation pattern variability and the impact of climatic change. We pay particular attention on assessing and illustrating the variability in how different catchments respond to different rainfall patterns and the impacts of climate change. The primary questions that we address are;

1. What is the relative importance of the storm pattern and volume of rainfall on urban flood peaks?
2. How will climate change affect storm patterns and volumes and what are the impacts on urban flood peaks?

Flood risk assessment and communication depend on flood risk mapping, for which flood inundation areas are needed (Merz et al., 2010). Urban catchments are typically complex and need to capture the response of the system along with the interactions of the various components of the stormwater infrastructure (Zoppou, 2001) to provide reliable flood depths to develop inundation areas. The main characteristic of stormwater in urban areas is that the flows are predominantly conveyed in constructed systems, replacing or modifying the natural flow paths. Including the complex hydraulics and possible hydraulic attenuation and timing of congruent flows will have an impact on flooding, particularly in developed environments. As discussed, temporal patterns of rainfall is now a critical aspect of design and planning of future storm systems. Research which uses temperature to project future rainfall and temporal patterns, and then assesses impacts on flooding has not been performed. This study aims to fill this research gap through an elaborate analysis of how rainfall intensities and patterns impact urban flood risk in a warmer climate.

2. Assessing flooding in developed/urban stormwater systems

Developed urban areas present the highest probability of causing damage and loss of life during flood events. There has been an increase in urban flooding in the past decade with densely populated developing countries like India and China coming into focus (Bisht et al., 2016; Zhou et al., 2017). A case study on the Oshiwara River in Mumbai, India has shown a 22 % increase in the overall flood hazard area due to changes in land use and increased urbanization within the catchment (Zope et al., 2016). In particular, flooding in Mumbai in 2005, which was caused by extreme rainfall coupled with inadequate storm sewer design, is blamed for 400 deaths (Bisht et al., 2016). China has also experienced a devastating flood season in 2016 (Zhou et al., 2016) with the rapid increase in urbanization. Even with better planned and mature urban cities, Europe and North America are not immune to flooding in urban areas (Ashley et al., 2005; Feyen et al., 2009; Smith et al., 2016). Impacts of climate change are expected to increase the risk of flooding and further exacerbate the difficulty of flood management in developed environments.

3 Assessing climate change impacts on flooding

The number of studies investigating climate change impacts on urban flooding is increasing as the importance of this topic is more and more recognized. However, research focusing on the impacts of climate change on precipitation temporal patterns remains limited. The majority of available research use Global Circulation Models (GCMs) and Regional Climate Models (RCMs) combined with statistical downscaling techniques to project IDF curves to reflect future climate conditions (Mamo, 2015; Nguyen et al., 2010; Schreider et al., 2000). For example Mamo (2015) used monthly mean wet weather scenario data projected by four GCMs for the period 2020-2055, along with historic data from 1985 to 2013, which were then used as weather generator input using LAR-WG, from which data was generated to develop revised IDF curves. Nguyen et al. (2010) used data sets generated by two separate GCMs to develop IDF and temporal patterns to reflect future rainfall patterns. The inconsistent results generated by the two different GCMs illustrate the challenge of forecasting future climate conditions with GCM generated results. It is recognized that GCM results form the largest part of the uncertainty in projected flood scenarios (Prudhomme and Davies, 2009).

Alternatively, research has shown that temperature, which influences the amount of water contained in the atmosphere, can have an impact on the patterns and total rainfall volumes of

storm events (Hardwick Jones et al., 2010b; Lenderink and van Meijgaard, 2008; Molnar et al., 2015; Utsumi et al., 2011; Wasko et al., 2015; Westra et al., 2013a). In general, intensification of rainfall events is expected with a trend towards 'invigorating storm dynamics" (Trenberth, 2011; Wasko and Sharma, 2015). Even though forecasts for climate change impacts on future flooding have a 'low confidence', global scale trends in temperature extremes are more reliable (Seneviratne et al., 2012). Following successful studies (Wasko and Sharma, 2017; Westra et al., 2013b) we take the approach of using temperature to project temporal patterns and rainfall volume to account for climate change impacts. As described in detail in section 5, we examine historical rainfall data coupled with daily average temperature to project temporal patterns and rainfall volumes to account for climate change impacts.

4. Study location, data and methodology

In this study we use temperature to project rainfall temporal patterns and volumes to evaluate the variability in flood risk as well as the impact to flood risk due to climatic change. Broadly, the steps followed are:

1. Apply multiple temporal patterns and rainfall volumes with their associated confidence limits in the H/H model to establish the variability in the flood risk
2. Develop scaling factors (Lenderink and Attema, 2015; Wasko and Sharma, 2015) for the volume and temporal pattern for future conditions using temperature as index
3. Evaluate the impact of temperature rise on flood risk by scaling temporal patterns for a temperature increase
4. Evaluate the cumulative impact of temperature rise on flood risk by scaling both volume and temporal patterns

The hydrologic and hydraulic modelling performed here used the EPA-SWMM model of an urban/suburban catchment in Minneapolis, Minnesota, USA. The SWMM software package was initially developed by the United States Environmental Protection Agency (EPA, 2016) and has since been used as the base engine for most of the industry standard H/H modelling packages.

4.1 Study Location and model

The H/H model used in this study was developed for the South Washington Watershed District (SWWD) in the State of Minnesota, USA for the management of surface water flows and as well as for planning and management of on-going development work and capital

191 improvement projects. The catchment area of the SWWD is a highly developed
192 urban/suburban area and extends over 140-km^2. The model was initially built in the year
193 2000 and has been continuously maintained and updated with the latest available
194 landuse/land cover and stormwater infrastructure information. The model includes extensive
195 detail of all landuse types and stormwater infrastructures including sewers, culvert crossing,
196 open channel reaches, and constructed as well as natural storages. Highly detailed
197 delineation of both sub-catchment boundaries and impervious area was done using a high
198 resolution Digital Elevation Model (DEM), development construction and grading plan
199 overlays and aerial imagery within a GIS environment. All surface runoff is fed into the
200 appropriate inflow points of the hydraulic conveyance system. The model has been validated
201 and used to design major capital improvement and flood mitigation projects (Hettiarachchi et.
202 al. 2005, Hettiarachchi and Johnson, 2006). Additional model information is available in the
203 supplemental information section S1. For the purposes of this study and to reduce the
204 complexity and model run times, the model was trimmed to the upper section of the SWWD
205 representing an area of approximately 22 km2.

206 Figure 1 presents the focus areas along with the schematic of the model network to illustrate
207 the level of detail of the existing storm water infrastructure captured in the model. As
208 discussed above the model includes geometry details to explicitly model the street overflow
209 routes where flooding occurs as well as depth/area curves that capture flooding at the storage
210 nodes. This level of detail results in accurately modelling the travel time of flows within the
211 watershed and capturing all the runoff volume generated from the storm. Additionally, the
212 geometry detail provides a reasonably accurate representation of extents related to flooding.
213 The proper simulation of hydraulic attenuation and a variety of landuse types provide an ideal
214 platform for this study.

215 Table 1 lists the primary reference locations that are used for this study. The locations have
216 specifically been chosen to represent the range of possible conditions that are encountered in
217 urban catchments. The sub-catchment sizes vary from less than 0.5 km^2 to approximately
218 2 km^2, with an overall catchment of 22 km^2. Different land uses such as commercial and
219 industrial or different types of residential areas, as well as the amount of storage, have all
220 been considered. It is important to note that these locations were selected prior to any model
221 runs or availability of results and hence do not bias the results presented. Table 1 gives a
222 description of the primary landuse type of the subwatershed that drains to each reference
223 location along with the watershed area and the overall percentage of impervious surface area

within that watershed. It also describes if there are local storage ponds, either natural or constructed, that provide rate and volume control.

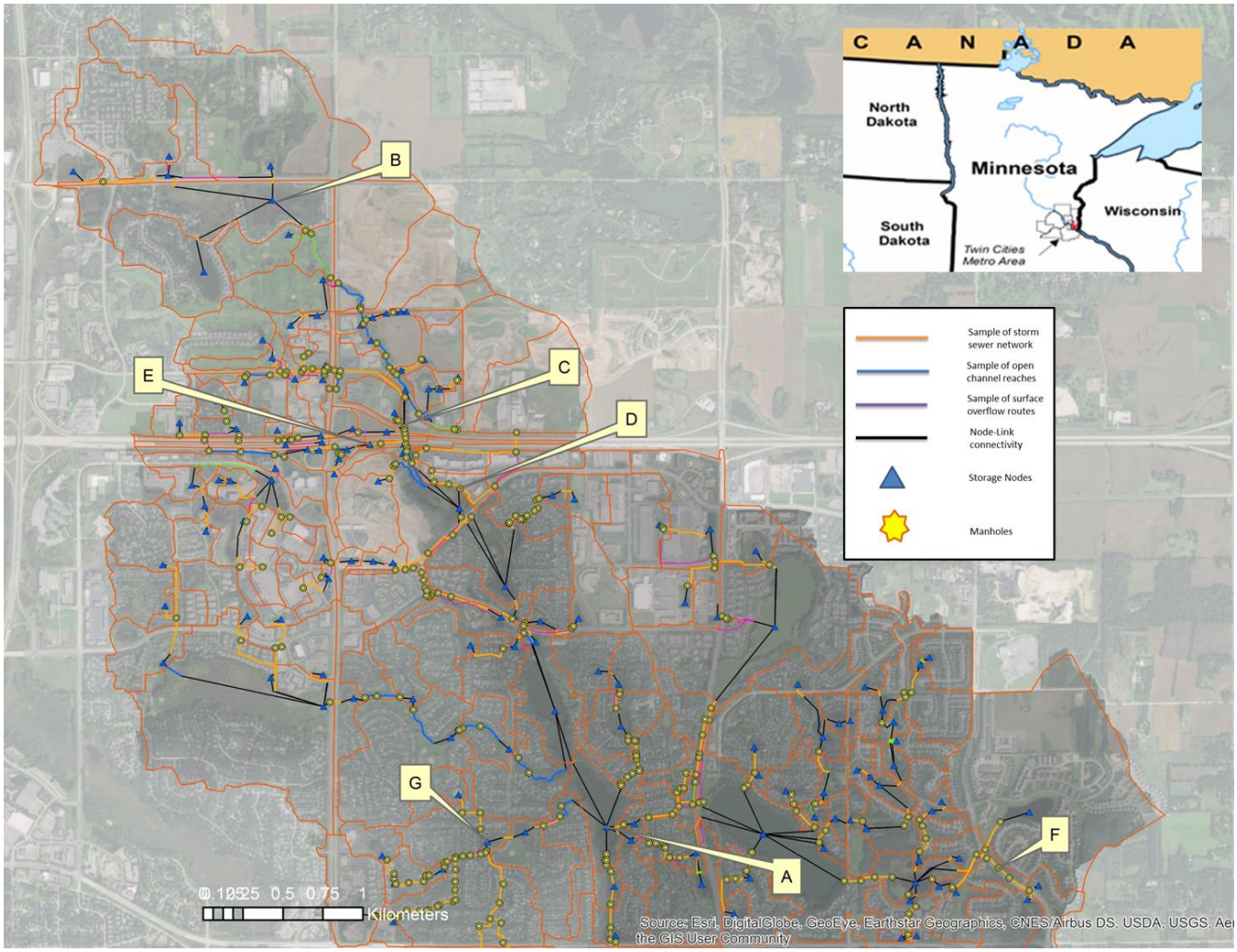

Figure 1 Location of the model and the sub-watersheds along with the reference points used in the discussion below. The details of the reference points and further explanation are presented in Table 1. The Orange links are example of the sewer network geometry in the model. The blue links represent reaches that are open channel. The magenta links are the surface overflow routes that capture flow that tends to flood in areas and spread outside the sewer network. The black links provides connectivity when the georeferenced locations of nodes are geographically different to the ends of some of the sewer network. The black links provide connectivity in the model.

238 **Table 1. Description of reference locations presented in Figure 1 and used to present results. Each**
239 **location represents a variation of landuse within the watershed**

Reference point	Landuse types and description	Watershed Area (km^2)	Average Percent impervious
(A) Wilmes	Natural lake and downstream limit of watershed.	~ 22	-
(B) Upstream	Predominantly rural, lower density residential landuse with good tree canopy and green spaces. Natural wetlands to mitigate flow with minimal to constructed storage	2.2	32
(C) Business park	Office space and parking lots with green space mixed in. Constructed storage and infiltration to help mitigate runoff	0.5	42
(D) Commercial 1	Retail and parking dominates this area with some green spaces added in. Minimal constructed storage. Two sub-surface infiltration basins installed under parking lots	.25	60
(E) Commercial 2	Retail and parking dominates this area with substantial constructed storage to help mitigate runoff rates and volumes. Part of the highway also drains through this point.	.75	48
(F) Residential 1	Medium density residential landuse with minimal constructed storage.	.35	24
(G) Residential 2	Medium density residential landuse with constructed storage.	1.05	39

240

241 ## 4.2 Precipitation and Temperature Data

242 The precipitation and temperature data used in the analysis were sourced from the National
243 Centers for Environmental Information hosted by the National Oceanic and Atmospheric
244 Administration (NOAA). Both hourly and daily rainfall data were downloaded from the
245 climate data online site for Minneapolis and St Paul (MSP) International Airport gauge,
246 which is the closest major airport to the study area. Daily data for the MSP airport was
247 available from 1901 through 2014, while hourly data was available from 1948 through 2014.

Daily maximum, minimum and average temperature data was also downloaded for the period from 1901 through 2014. For this analysis days that did not have precipitation data were assumed to have no rain.

The temporal patterns for storms and the depths of rainfall were taken from NOAA ATLAS 14 volume 8 (Perica. et. al. 2013) – the current state of the art design standard for this location. The modelling analysis centred on the 50-year (2% exceedance probability) storm, which is a total rainfall volume of 160 mm in 24-hours, for the area within the SWWD in the USA. The 90 % confidence margin storm depths were added to the analysis to look at how modelled flood depths vary with total precipitation (Table 2). Six temporal distributions (two patterns with their associated confidence margins) were chosen from NOAA ATLAS 14 volume 8 to investigate how flood depths are impacted by the shape of storm over a 24-hour period. Table 2 describes the different storm temporal patterns and each of the precipitation volumes modelled. The spatial distribution of rainfall is assumed to be uniform for this study. Even though we acknowledge that spatial variability of rainfall can have an impact on flooding, adding that dimension to the current analysis would have made the level of effort excessive. Also, by not spatially varying the rainfall distribution, we are able to better focus on the sensitivity of temporal patterns on flooding impacts.

Table 2. Description of notation used in reference to the modelled storm depths and temporal distributions (NOAA Atlas 14 volume 8 appendix 5 accessed from http://www.nws.noaa.gov/oh/hdsc/PF_documents/Atlas14_Volume8.pdf)

Design Rainfall	Description
160 mm 24 hour	2 % exceedance 24-hour duration (50-year return period) rainfall depth
125 mm 24 hour	Lower margin of the 90% confidence interval of the 2 % exceedance 24-hour duration (50-year return period) rainfall depth-Approximately Equivalent to the 20-year 24 hour ARI
210 mm 24 hour	Upper margin of the 90% confidence interval of the 2 % exceedance 24-hour duration (50-year return period) rainfall depth-Approximately Equivalent to the 200-year 24 hour ARI
Temporal pattern	**Description**
Q1-10 - (a)	NOAA Midwest region, 1st quartile 10th percentile temporal distribution
Q1-50 - (b)	NOAA Midwest region, 1st quartile 50th percentile temporal distribution
Q1-90 - (c)	NOAA Midwest region, 1st quartile 90th percentile temporal distribution
Q3-10 - (d)	NOAA Midwest region, 3rd quartile 10th percentile temporal distribution
Q3-50 - (e)	NOAA Midwest region, 3rd quartile 50th percentile temporal distribution
Q3-90 - (f)	NOAA Midwest region, 3rd quartile 90th percentile temporal distribution

The quartiles indicate the timing of the greatest percentage of total rainfall that occurs during a storm. First quartile indicates that the majority of the rainfall, including the peak, occurs in the 1st ¼ of the duration, which is between hours 1 through 6 in the case of a 24-hour storm. Third quartile indicates that the majority of the rainfall, including the peak occurs in the 3rd quarter of the storm duration, that is, hours 12 through 18 in the case of a 24-hour storm. The temporal distributions were also separated in Atlas 14 to determine the frequency of occurrence within each quartile to determine a percentile for each distribution.

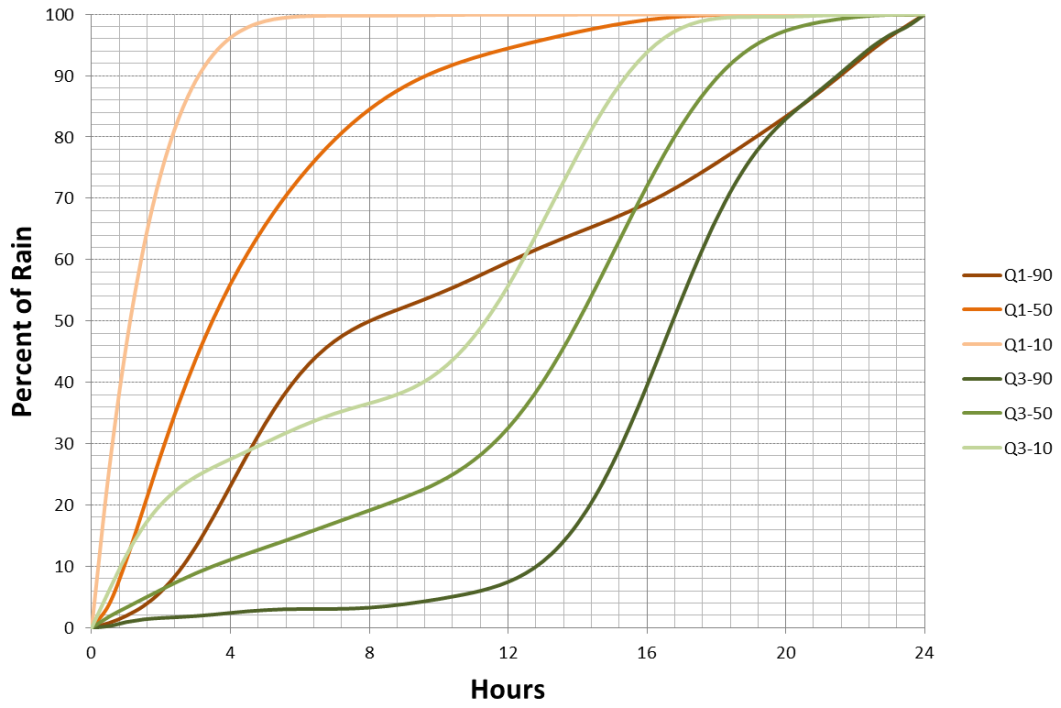

Figure 2. NOAA Atlas 14 temporal patterns used in the modelling

The SWMM model was run for each of the precipitation amounts for the six temporal patterns, a total of 18 model runs, to generate the base dataset for current conditions and establish the variability in the current climate. The impact of climate change due to changed temporal patterns was assessed by modelling the 2% exceedance rainfall value (160 mm) with temporal patterns scaled for an expected temperature increase. Finally the cumulative impacts of changed temporal patterns and volume were evaluated by scaling both the rainfall volume and temporal patterns with temperature. An important point to note is that only the rainfall time series was changed appropriately for each model run. All the boundary conditions such as initials water levels at storage locations and all hydrologic parameters for each of the above model runs were kept the same for every model run.

4.3 Temperature scaling of temporal patterns and rainfall volume

To assess the impact of climate change, design storm temporal patterns and rainfall volumes need to be projected for a future warmer climate. Most methods that project rainfall for future climates focus on downscaling output from general circulation models to those required for hydrological applications (Fowler et al., 2007; Maraun et al., 2010; Prudhomme et al., 2002) through either dynamical or statistical models (Wilks, 2010). Downscaling methods,

however, will not replicate design rainfall (Woldemeskel et al., 2016), so an attractive alternative is that proposed by Lenderink and Attema (2015) whereby historical temperature sensitivities (scaling) are directly applied to the design rainfall. Here, we assume that temperature is the primary climatic variable associated with changing rainfall. This is consistent with studies that find that temperature is a recommended covariate for projecting rainfall (Agilan and Umamahesh, 2017; Ali and Mishra, 2017) and temperature sensitivities implicitly account for dynamic factors (Wasko and Sharma, 2017). Indeed projecting rainfall directly using temperature sensitivities gives comparable results to more sophisticated methods of rainfall projection using numerical weather prediction (Manola et al., 2017).

Using established methods (Hardwick Jones et al., 2010a; Utsumi et al., 2011; Wasko and Sharma, 2014), the volume scaling for the 24 hour storm duration was calculated using an exponential regression. The results are presented in Figure 5. First, daily rainfall was paired with daily average temperature. The rainfall-temperature pairs were binned on 2ºC temperature bins, overlapping with steps of one degree. For each 2ºC bin a Generalized Pareto Distribution fitted to the rainfall data in the bin that was above the 99th percentile to find extreme rainfall percentiles (Lenderink et al., 2011; Lenderink and van Meijgaard, 2008). Extreme percentiles below the 99^{th} percentile (inclusive) were calculated empirically. A linear regression was subsequently fitted to the fitted log-transformed extreme percentiles and used as the rainfall volume scaling (Figure 5). Hence the volume (V) is related to a change in temperature (T) by

$$V_2 = V_1(1 + \alpha)^{\Delta T}$$

Where α is the scaling of the precipitation per degree change in temperature.

Temporal pattern scaling was calculated using hourly data, again paired to the average daily temperature and followed the proposed methodologies in (Wasko and Sharma, 2015). The largest 500 storm bursts of duration 24 hours were identified in the hourly data, with each storm burst independent (not overlapping). The 24-hour duration storm bursts were divided into 6 fractions, each fraction with duration of four hours. Each fraction was divided by the rainfall volume and ranked from largest to smallest. An exponential regression was fitted to the fractions corresponding to each rank and their corresponding temperature to produce a temporal pattern scaling. The scaled temporal patterns were then applied and run through the H/H models.

5 Results and Discussion

The results from the modelling analysis is presented and discussed below. We show that the current temporal patterns for design flood estimation need to be adjusted to account for climate change impacts as do design rainfall volumes.

5.1 Temporal patterns and volume scaling

The scaling of the temporal pattern fraction for Minneapolis is presented in Figure 3. Table 3 provides the scaling that results from the fitted regression in each of the panels in Figure 3. A temperature change of 5°C was selected to determine the percentage change based on temperature increases estimated for the RCP8.5 scenario in Figure SPM7(a)(IPCC 2014) projected for 2081-2100. The selection of the RCP8.5 scenario was based on the goal of this paper to demonstrate the importance of accounting for climate change in rainfall patterns as well the current literature suggesting that we are tracking on a RCP8.5 scenario (Peter et al., 2013). Additional analysis performed for the RCP4.5 scenario (supplemental information section S2) shows similar trends in results but of a lesser magnitude. It is important to note that rigorous thought is needed on how far out and what level of climate impacts should be considered when selecting a threshold for design or when setting absolute flood depths.

As the slopes in Figure 3 and factors in Table 3 show, only the first fraction scaled positively, which means that the 4 hours that included the highest amount of rainfall scale up while the remaining rainfall fractions scale down. The results are consistent with "invigorating storm dynamics" (Lenderink and van Meijgaard, 2008; Trenberth, 2011; Wasko and Sharma, 2015; Wasko et al., 2016b) resulting in a less uniform, more intense storm. The percentage adjustments were normalized to make sure that total rainfall amount did not change from the current value of 160 mm in 24-hours. Figure 4 presents (Q1-50 and Q3-50 shown as an example) the changes to the temporal patterns when the scaling percentages calculated above are applied. Figure 4 illustrates the change to the highest peak rainfall rate and the decrease in the rest of the rainfall fractions. Similar scaling was applied for all six temporal patterns that were used in the H/H modelling analysis. As an additional verification, a similar analysis was completed for two neighbouring locations (Sioux Falls South, Dakota and Milwaukee, Wisconsin). The fraction and volume scaling results for both Sioux Falls and Milwaukee were consistent with those discussed in this paper.

Figure 5 presents the precipitation volume temperature pairs, the extreme percentiles generated based on the temperature bins, as well as the resulting scaling for the 24 hour rainfalls. The daily total rainfall of 160 mm fell into the 99.99th percentile based on a cursory ranking of the daily precipitation data. Hence, the 99.99th percentile 4.7 % scaling was selecting for the 24 hour volume. This is broadly consistent with Utsumi et al. (2011) and Wasko et al. (2016a) who present scaling between 2 and 5 % for the central north of the U.S for the 99th percentile and throughout Australia and less than the scaling found by Mishra et al. (2012) who used hourly precipitation, which is consistent with the expectation that shorter duration extremes have greater scaling (Hardwick Jones et al., 2010a; Panthou et al., 2014; Wasko et al., 2015). This value also appears to be consistent both with historical trends and climate change projections. Barbero et al (2017) looked at a non-stationary extreme value analysis and found a sensitivity of approximately 7%/ºC for a non-stationary Theil-Sen estimator for North America. Globally, Westra et al. (2013) find historical trends have global sensitivity between 5.9%/ºC and 7.7%/ºC. However, Kharin et al (2013) report an approximately 4% sensitivity over land globally from the CMIP5 model results with a range of 2.5-5% for the U.S.A. Relative to the literature stated above we believe our projections are consistent with the available evidence regarding precipitation change.

This 4.7 % scaling converts to an approximately 20 % increase in the volume of rainfall in a 24 hour period for a five degree increase. Applying the 20 % increase to the 160 mm in 24-hours gives a rainfall depth of 208 mm in 24 hours. Coincidentally, 208 mm (~210 mm) in 24 hours is the upper margin of the 90% confidence interval for the 160 mm event based on the margin provided in NOAA Atlas 14.

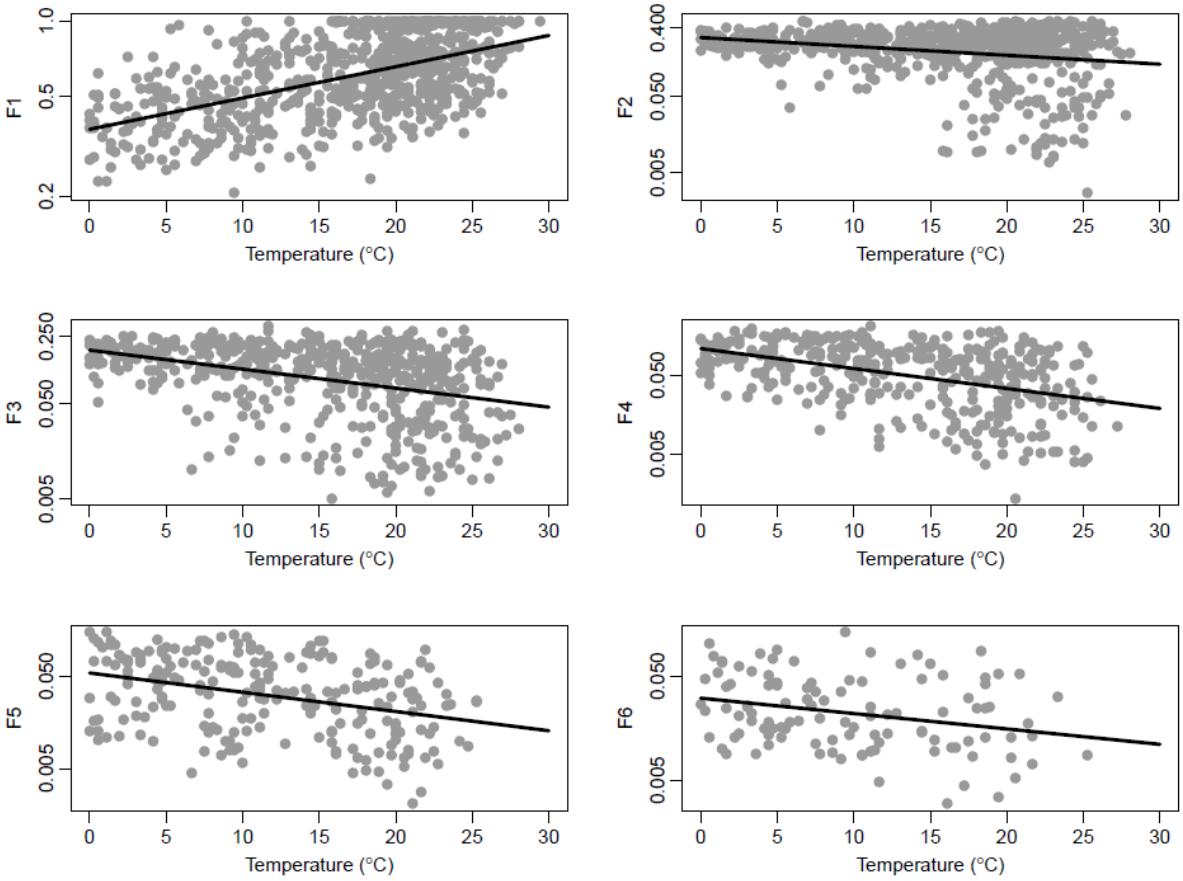

389

390 **Figure 3. Scaling temporal pattern fractions with temperature for Minneapolis (1948-2014 hourly data).**
391 **Black lines represent the fitted exponential regression. F# represents the # ranked fraction.**

392 **Table 3 Temporal pattern scaling factors for each of the fractions**

Fraction	Scaling factor
F1	0.029
F2	-0.026
F3	-0.045
F4	-0.057
F5	-0.047
F6	-0.033

393

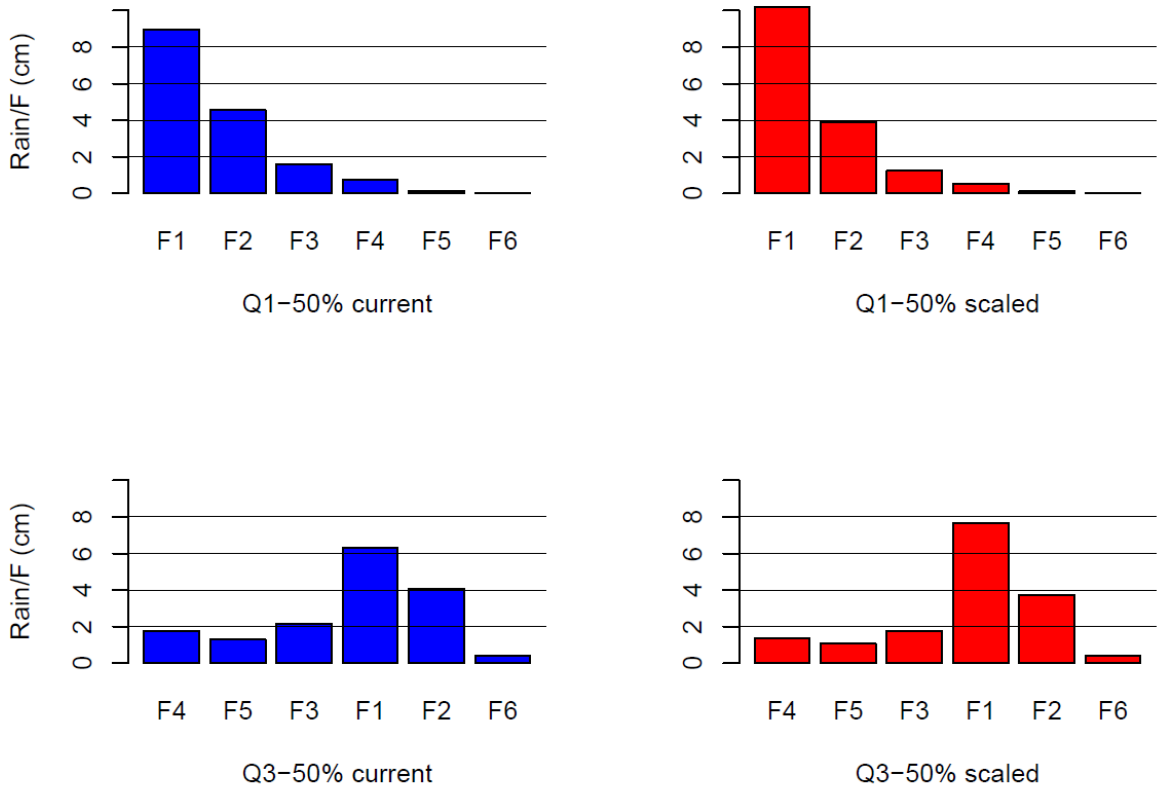

394

395 **Figure 4 Q1-50 and Q3-50 temporal patterns projected for temperature rise of 5^0 C. Total rainfall of 160**
396 **mm over 24 hours with each fraction representing accumulated rain for 4-hour periods.**

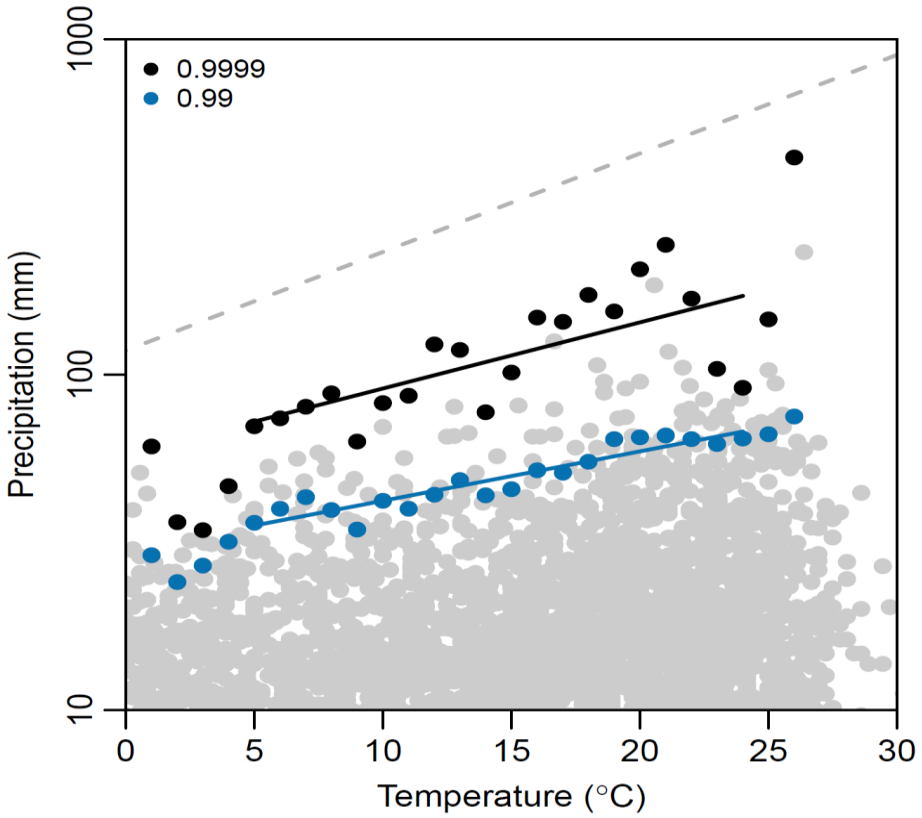

.

Figure 5 Scaling total volume of rainfall with temperature for Minneapolis (1901-2014 daily rainfall). Grey dots are rainfall temperature-pairs and the coloured dots are the extreme percentiles. The grey dashed line represents a scaling of 7 %.

5.2 Flood depth response to temporal patterns and total rainfall variability.

The hydrologic/hydraulic model was run for the 18 different combinations of rainfall volumes and temporal patterns. Results are presented for the five reference locations throughout the watershed representing different landuse types that are typical in a developed area as described in Table 2. The selection of the reference points essentially provides results at different sub-catchments, or different sub-models. These sub-models show the variation in catchment response to runoff generated by a variety of land use types as well as changes in how the flows move through the different stormwater infrastructure.

Figures 6(a) shows the depth/time curve at Wilmes Lake (location A) which is the main regional collection point and the downstream end of the model. Each curve represents change in depth versus time for the six temporal patterns distributing the same total rainfall volume of 160 mm. The differences in shape, peak flood depth and the time to peak illustrate the variability in catchment response that can result purely due to variation in rainfall pattern during a storm event. A striking result is the approximately 1.3 m variation in flood depth at Wilmes Lake purely due to variation of how the rain falls within the duration of the storm. The highest flood depth curve is a result of the most intense storm event pattern which is the Q1-10 distribution. The depth at Wilmes Lake rises quickly during the Q1-10 event but the peak flood depth still occurs within the 40 – 60 hour band similar to the other rainfall patterns. The high intensity of the Q1-10 pattern can overwhelm local conveyance and storage structures, resulting in overflows that flushes down to the low lying areas rapidly, causing the water level at the lake to rise. Note that the next highest peak flood level results from the Q3 patterns which has the majority of the precipitation loaded at the latter half of the storm event. Comparison of the total runoff volume generated during each model run f for the catchment between Q1-50 to Q3-50 temporal patterns shows a 9.5% increase (refer to table 4 in supplemental information) for the same 50 year (160 mm in 24 hours) storm event. A third quartile rainfall pattern can results in higher runoff volume as the soil saturates and infiltration rates are reduced and can cause worse flooding as local storage structures and ponds fill up by the time the bulk of the storm occurs. The results for the Q-3 patterns suggests that regional storage facilities such as Wilmes Lake within the SWWD are more sensitive to the runoff volume than the instantaneous peak flow rate, and thereby more sensitive to end loaded temporal patterns during storms.

Figure 6(b) illustrates the same type of variation of peak flood depth due purely to the different temporal patterns at all of the reference points. Locations A, C, D and G average about a metre in peak flood depth variation. When considering that the typical freeboard (added elevation above base flood elevation) used in the USA when setting lowest open elevations for structures is 0.65 m, a 1 m variation in peak flood elevation is significant. As described in Table 1, the landuse within the subcatchment that drains to location B is rural with local natural storage whereas locations C and D have commercial land use with higher impervious land cover. This difference in land cover can explain why the variability in peak flood depth relative to changes in temporal patterns is lower at approximately 0.5 m and suggests that catchments with higher impervious surfaces have a higher sensitivity to rainfall

443 patterns. Additionally, locations F is within the storm sewer system which suggests that
444 variation in flow rates, or peak runoff from a catchment, does not always translate to higher
445 variation in flood depths.

446 The depth vs time curves in Figure 6(a) also illustrate the value of including detailed
447 hydraulic routing in the modelling analysis. As an example, the curves for Q1-10 and Q3-90
448 patterns show the difference of catchment response due to a high intensity rainfall event that
449 results in an initial peak flood depth resulting from overflows followed by the lagged
450 response of the volume accumulation compared to the scenario of higher volume of runoff
451 due to saturated soils. The variability in how the catchment responds to different temporal
452 patterns is consistent with studies by Ball (1994) and Lambourne and Stephenson (1987).
453 Though these studies focused primarily on the hydrologic aspect of the modelling and peak
454 flow rates and volumes, the variation in catchment response to changes in "how it rains" is
455 similar. The current study has the added benefit of detailed hydraulics routing and it is
456 reasonable to assume that using only hydrologic routing, which is more common in current
457 literature, would not have captured some of the detailed environmental hydraulics that can
458 lead to better flood estimates in developed environments.

459

460

461

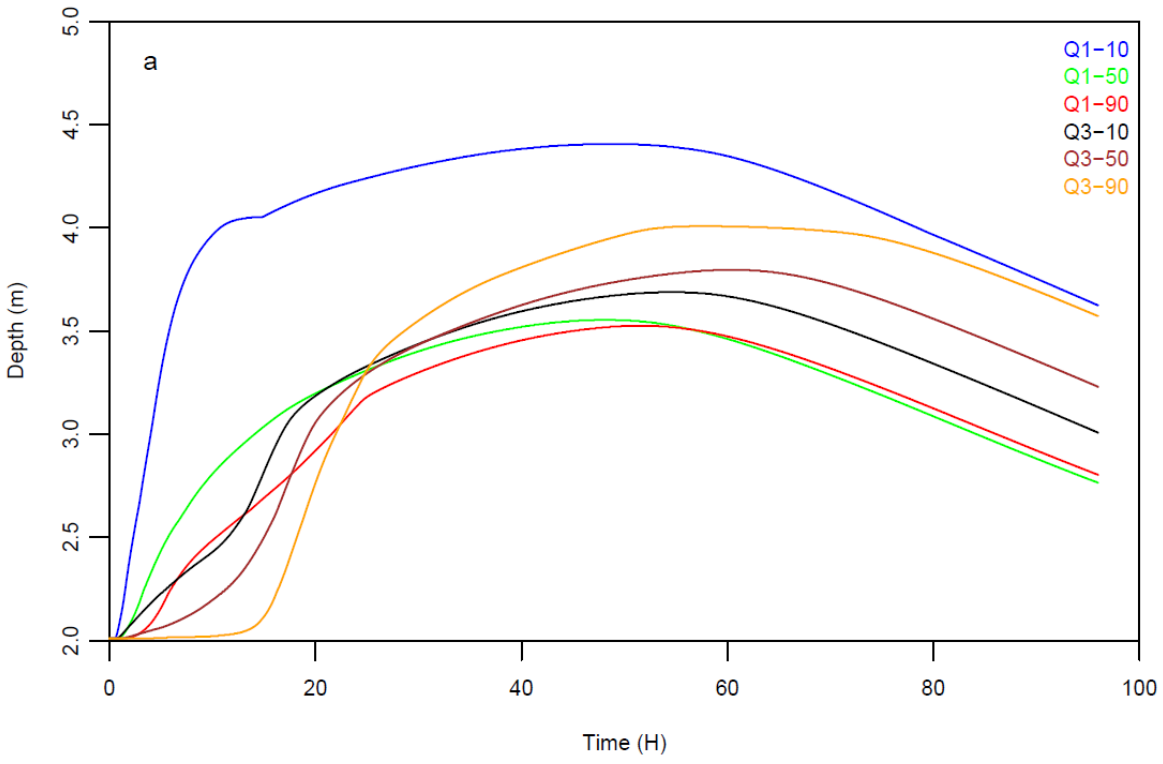

462

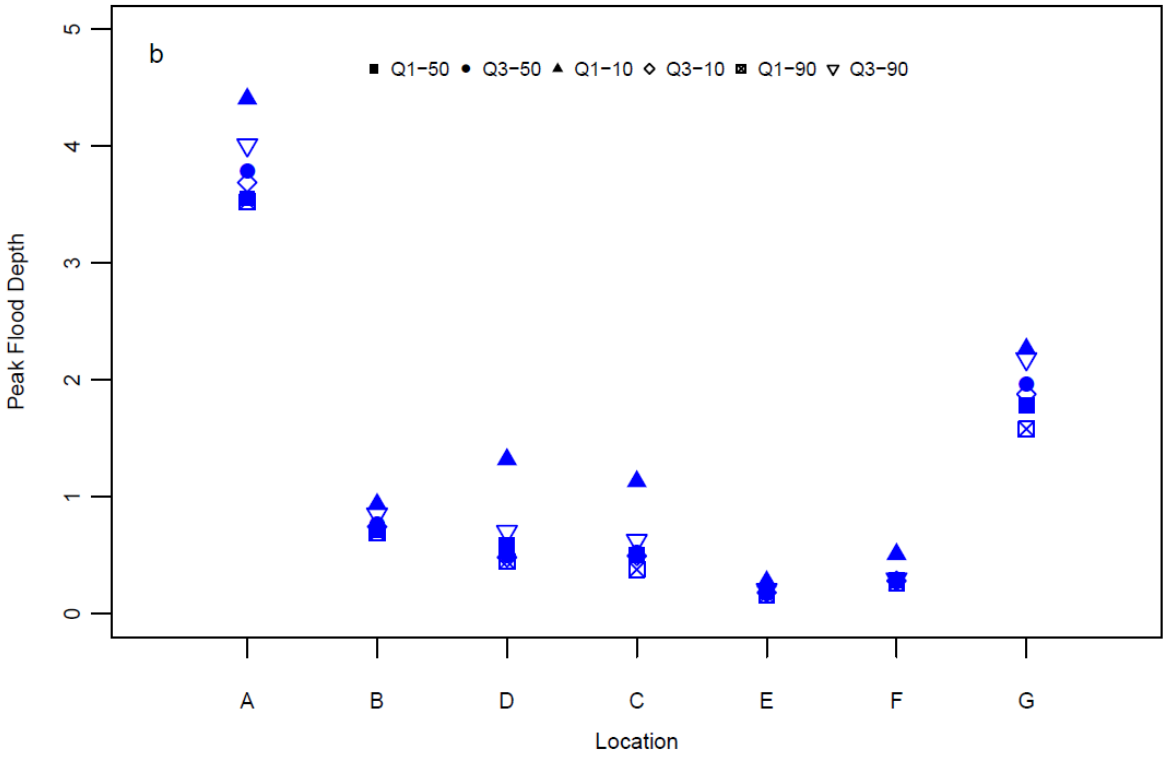

463

464 **Figure 6 (a) Depth over time at Wilmes Lake (Location A), which is the downstream regional reference**
465 **point in Figure 1. Depth vs time curves are plotted for 160 mm of total rainfall over 24 hours with the six**
466 **temporal patterns. (b) Presents the variation of peak flood depth (m) at reference locations throughout**

the watershed (ref to table 1) with variation of temporal patterns for a total of 160 mm of rainfall over 24 hours.

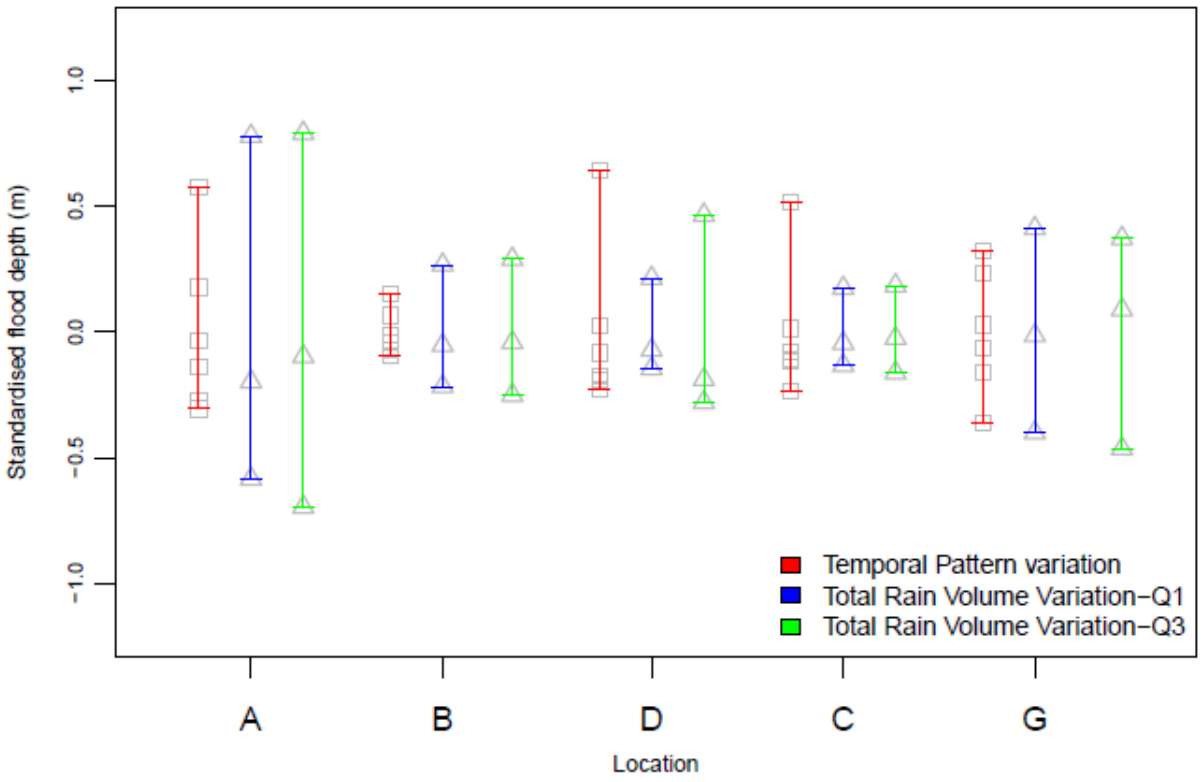

Figure 7 Comparison of total volume of rainfall and temporal patterns variability impact on peak flood depth. Flood depth variation due to the 6 different temporal patterns with 160 mm of rain compared to 110, 160 and 210 mm of total rainfall over 24 hours distributed over Q1-50 and Q3-50 temporal patterns. Flood depths were standardised by subtracting the mean at each location for ease of comparison.

One of the primary questions that we set out to answer was the comparison of "how it rains" versus "how much it rains". For clarification, "how it rains" refers to the variation of temporal patterns during a storm event with the total rainfall volume with the 24 hours held constant. The term "how much it rains" refers to different volumes of total rainfall within 24 hours for each storm event with the temporal pattern held constant. Figure 7 makes the direct comparison between the variations of peak flood depth between "how it rains" versus "how much it rains". The range in peak depths at the reference locations indicates how the different catchments respond to variability in storm volume and pattern.

Comparison of the range of peak flood depths at locations C and D indicates a higher sensitivity to variation in "how it rains" as opposed to changes "how much it rains". Conversely, locations A, B and G indicate a higher range in flood depths due to changes in

total rainfall volume, or "how much it rains" compared to changes in temporal patterns, or "how it rains". Even though one can note that locations C and D receive runoff from catchments that have a majority of higher impervious landuse relative to other locations, the number of data points does not allow for a statistically significant comparison of the sensitivity of impervious percentages in landuse to the difference in "how it rains" vs. "how much it rains". But it is important to note the consistency in the range of results across all the locations and the fact that "how it rains" has as much of an impact in the peak flood depths as "how much it rains". The results in Figure 7 clearly answer the first question presented in the introduction that temporal patterns of storms are as important as the total volume of rainfall during a storm in watershed response and flood estimation.

The results presented in Figures 6 and 7 shows that temporal patterns, or "how it rains" add a degree of variability and has a significant contribution to the overall uncertainty in H/H modelling results. This is especially a concern given the evidence to date that systematic change is occurring to rainfall patterns across climate zones, making them more intense and impactful in derived flood estimations (Wasko and Sharma, 2015). The added variability has implications on the already complex nature of properly accounting for uncertainty in flood forecasts or the impacts of climate change in future flooding conditions, which can in turn have implications on how society will accept the socio-economic impacts of adaption as previously mentioned. Hence, careful consideration of "how it rains" and changes in "how it rains" have to be included in any H/H modelling frame work along with the current typical practice of modelling "how much it rains".

5.3 Impact of applying temperature scaling to temporal patterns and rainfall volume on flood depths

Figure 8 compares the results for projected temporal patterns with results from the base simulation. Both scenarios are based on the 50 year return period event which is 160 mm distributed over the six base and projected temporal patterns. The results shown in Figure 8 are variation of the peak flood depth around the mean of the results from the base conditions models. In other words, the results were standardized by subtracting the mean of the base conditions from the results at each location.

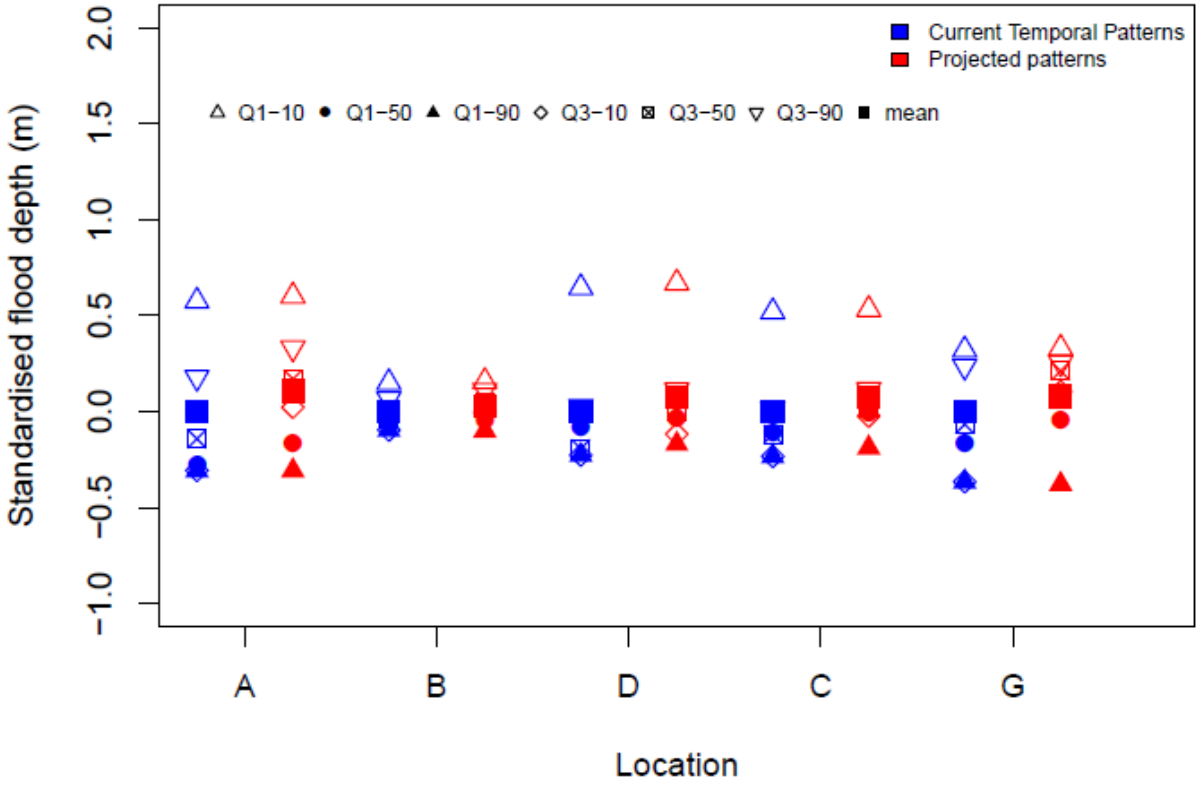

Figure 8. Impact of rise in temperature on the peak flood depth variation at reference locations within the watershed when scaling is applied only to temporal patterns. The peak flood depths at each reference point are based on 160 mm of total rain distributed over the 6 temporal patterns used. Temperature scaling (T/S) for the temporal patterns are based scaling fractions presented in Figure 3. Flood depths were standardised by subtracting the mean from the base simulations presented in Figure 6 for each location. The mean flood depth is shown as solid squares.

As expected, the highest flood depth results from the Q1-10 pattern for both current and scaled conditions. But the results at the highest depths show little change due to temperature scaling of the Q1-10 pattern. The Q1-10 pattern is an extremely high intensity event with majority of the rainfall occurring in the first fraction of the event. Applying the scaling percentages to this fraction makes minimal changes to the overall pattern of rainfall resulting in no appreciable change in peak flood depths. If we take the extreme Q1-10 event out of consideration, one can say that qualitatively there is an increasing trend in flood depths due to changes in the projected temporal patterns. The important fact is that these plots are based on the same total rainfall volume of 160 mm. The moderate increasing trend in the results is purely due to the projected temporal patterns. As discussed previously, location B represents a more rural type catchment and shows less sensitivity to changes in rainfall patterns.

Figure 9 shows the same comparison as in Figure 8 when temperature scaling is applied to both the temporal pattern and rainfall volume. Hence Figure 9 presents the cumulative impacts of temperature scaling to the base conditions. As in Figure 8, the results in Figure 9 show the variation of results for both scenarios around the mean of the base condition flood depth at each location.

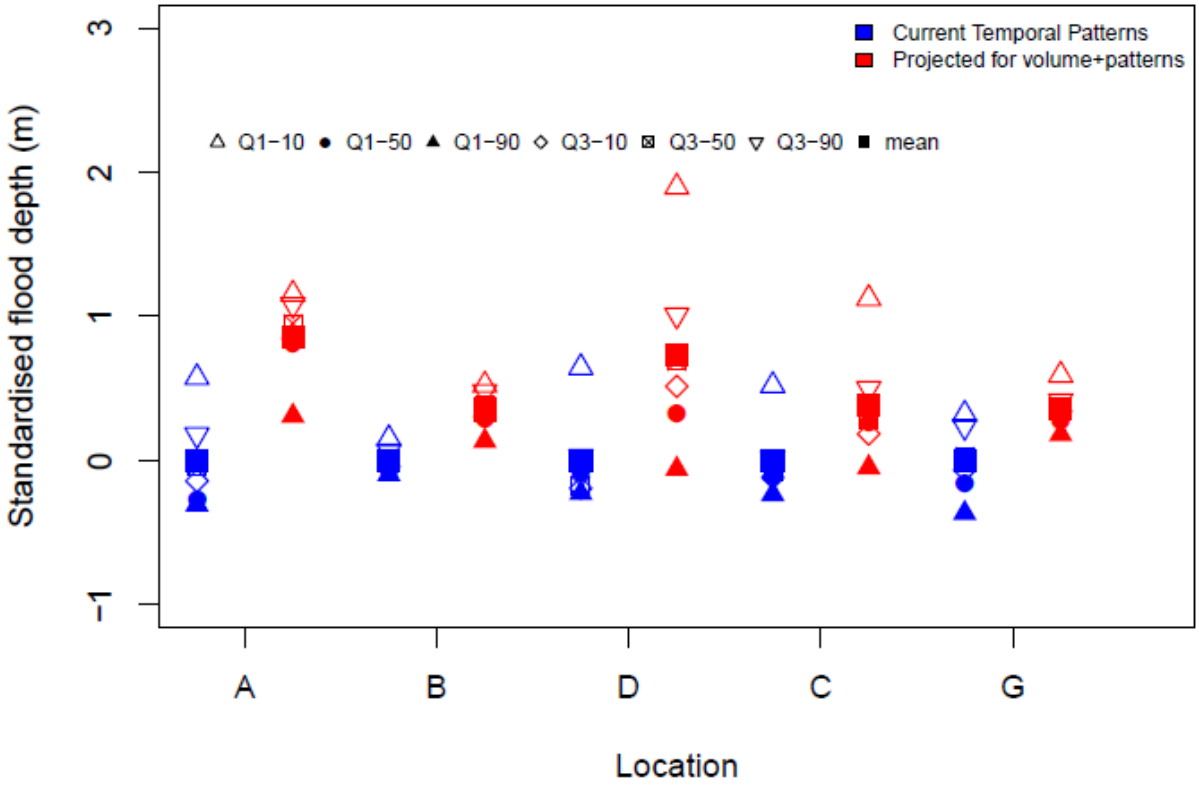

Figure 9. Impact of rise in temperature on the peak flood depth variation at reference locations within the watershed, when scaling is applied to both rainfall volume and temporal pattern. The peak flood depths at each reference point are based on 210 mm of total rain distributed over the 6 temporal patterns used. Flood depths were standardised by subtracting the mean from the base simulations presented in Figure 6 for each location. The mean flood depth is shown as solid squares.

As expected, substantial increase in flood risk is seen when the cumulative impacts of changes to temporal pattern and increase in precipitation volume due to temperature rise are modelled. The mean flood depth is outside the upper margin of the highest flood depth for base conditions except at the business park (C). The business park location (C) comes close to meeting this threshold as well. The mean flood depth at Wilmes Lake (A) increases by approximately 1 m, which translates to a significant increase in the extent of flooding. The biggest change due to cumulative impacts occurs at the upstream location (B) were

552 previously, when only the temporal patterns were scaled, minimal impact was shown. The
553 increase in flood depth at the reference locations due to changes to temporal patterns alone
554 range from 1 % to 35 %, while the cumulative impacts increase flood depth from 10 % to as
555 much as 170 %. These results are similar to Zhou et al. (2016) who projects a 52% increase
556 in urban flooding for an RCP 8.5 scenario in China. When considering all the nodes in the
557 model, the average increase in flood depth due only to changes in temporal patterns was 6 %.
558 The average increase in flood depth throughout the entire model due to cumulative impacts of
559 both changes to temporal pattern and rainfall volume is 37 %. The percentage increase
560 (Table S2) shows that there is a significant impact to overall flood risk throughout the
561 catchment and that it is not isolated to the reference points that are discussed in detail. These
562 results clearly show the increasing trend along with the significant variability in flood risk in
563 developed environments.

564 Additionally, the range of the results and hence the overall variability has increased at the
565 commercial and business park areas (C, D) locations when compared to Figure 8. But this
566 change in the range is not consistent throughout the catchment. The higher intensity and the
567 larger total volume of rainfall overwhelm the existing infrastructure with much larger surface
568 overflows in different ways depending on the site and extents. Also, the amount of increase
569 in the flood depths can change at different locations as the flooding increases. The changes
570 to the range of depths as seen in Figure 9 suggests that quantifying and accounting for
571 uncertainty in flood forecasts becomes more complex for future climates.

572 The use of detailed hydrologic and hydraulic modelling provides some of the nuances in
573 catchment response that adds important details to the results and our understanding on the
574 impacts of temporal patterns to flood risk, such as higher intensity rainfall does not always
575 results in the higher flood risk. The variation of reference locations selected for this study
576 provides a reasonable assessment of how the flows interact with the physical features of the
577 catchment and how the results differ based on the location and features. This study clearly
578 shows the sensitivity of the catchment to variation in how it rains, in particular the areas that
579 are more impacted by volume as opposed to flow rate. Explicitly including intensification of
580 rainfall patterns and volume due to climate change along with detailed H/H modelling to
581 assess the variability in catchment response makes this study unique among available
582 literature. The methodology presented here is universally applicable and the benefits of
583 correctly designing infrastructure are likely to far outweigh the cost of the added effort, even
584 in industry applications.

6 Conclusions

The significance of temporal patterns and how climate change impacts on rainfall patterns affect flooding in developed environments was investigated using detailed hydrologic and hydraulic modelling. Climate change impacts were undertaken by projecting historical precipitation-temperature sensitivities on storm volumes and temporal patterns. The following conclusions can be drawn from the results presented;

1. The response of a complex catchment is sensitive to variability in rainfall temporal pattern. The flood depths varied in excess of 1 m at Wilmes Lake when different temporal patterns were used with a constant volume of precipitation.
2. The variability of peak flood depth due to temporal pattern had similar magnitude when compared to variability due to total rainfall volume, which clearly shows that the temporal pattern of rainfall, or "how it rains" is as important as the volume of rainfall or "how much it rains" for the purposes of H/H modelling.
3. Temporal patterns add a quantifiable variability to the results generated in H/H modelling and need to be carefully considered when presenting results and associated uncertainties.
4. The temporal patterns intensified when scaled based on estimated temperature increases due to climate change.
5. A 1 % to 35 % increase in flood depth resulted when the scaled temporal patterns were used in the H/H model, suggesting an increase in potential flood risk purely due changes to "how it rains" as a result of climate change impacts.
6. A 10 % to 170 % increase in flood depth resulted when the projected rainfall volume was added to the projected temporal patterns, which shows a substantial increase in flood risk as a results climate change impacts on rainfall.
7. The variability of flood depth increased after temporal patterns and rainfall volumes were projected suggesting that H/H modelling for future planning and design needs to give serious consideration to the aspects of variability of rainfall patterns as well as increase in rainfall amounts.
8. Regional storage facilities are sensitive to rainfall patterns that are loaded at the latter part of the storm duration while the extremely intense storms will cause flooding at all locations.

The effect of projected intensification of storms due to climate change impacts suggests that action needs to be taken promptly to prevent flood damages and possible loss of life. The two most important points that can be derived from this study is that temporal patterns and storm volumes need to be adjusted to account for climate change when applying to models of future scenarios. The general application of H/H modelling analysis needs to adopt an ensemble approach rather than a single event model to consider the significant variability in rainfall patterns that can generate a substantial range in results in order to make a properly informed decision as demonstrated here.

Acknowledgments

The authors acknowledge and thank the South Washington Watershed District (http://www.swwdmn.org) in Minnesota, USA for providing the model as well as the background data used for the analysis. We also acknowledge financial support of the Australian Research Council. The rainfall and temperature data for Minneapolis Airport and locations around the site were taken from https://www.ncdc.noaa.gov/cdo-web/. NOAA Atlas 14 Volume 8 is available at http://www.nws.noaa.gov/oh/hdsc/PF_documents

Technical details of EPA-SWMM can be found at https://www.epa.gov/water-research/storm-water-management-model-swmm.

References

Adams, B. J. and Howard, C. D.: Design storm pathology, Canadian Water Resources Journal, 11, 49-55, 1986.

Adger, W. N., Agrawala, S., Mirza, M. M. Q., Conde, C., o'Brien, K., Pulhin, J., Pulwarty, R., Smit, B., and Takahashi, K.: Assessment of adaptation practices, options, constraints and capacity, Climate change, 2007. 717-743, 2007.

Adger, W. N., Dessai, S., Goulden, M., Hulme, M., Lorenzoni, I., Nelson, D. R., Naess, L. O., Wolf, J., and Wreford, A.: Are there social limits to adaptation to climate change?, Climatic Change, 93, 335-354, 2009.

Agilan, V. and Umamahesh, N.: Modelling nonlinear trend for developing non-stationary rainfall intensity–duration–frequency curve, International Journal of Climatology, 37, 1265-1281, 2017.

Alexander, L. V., Zhang, X., Peterson, T. C., Caesar, J., Gleason, B., Tank, A. M. G. K., Haylock, M., Collins, D., Trewin, B., Rahimzadeh, F., Tagipour, A., Kumar, K. R.,

Revadekar, J., Griffiths, G., Vincent, L., Stephenson, D. B., Burn, J., Aguilar, E., Brunet, M., Taylor, M., New, M., Zhai, P., Rusticucci, M., and Vazquez-Aguirre, J. L.: Global observed changes in daily climate extremes of temperature and precipitation, Journal of Geophysical Research: Atmospheres (1984–2012), 111, 2006.

Ali, H. and Mishra, V.: Contrasting response of rainfall extremes to increase in surface air and dewpoint temperatures at urban locations in India, Scientific Reports, 7, 1228, 2017.

Ball, J. E.: The influence of storm temporal patterns on catchment response, Journal of Hydrology, 158, 285-303, 1994.

Barbero, R., Fowler, H. J., Lenderink, G., and Blenkinsop, S.: Is the intensification of precipitation extremes with global warming better detected at hourly than daily resolutions?, Geophysical Research Letters, 44, 974-983, 2017.

Bisht, D. S., Chatterjee, C., Kalakoti, S., Upadhyay, P., Sahoo, M., and Panda, A.: Modeling urban floods and drainage using SWMM and MIKE URBAN: a case study, Natural Hazards, 84, 749-776, 2016.

Cameron, D.: An application of the UKCIP02 climate change scenarios to flood estimation by continuous simulation for a gauged catchment in the northeast of Scotland, UK (with uncertainty), Journal of Hydrology, 328, 212-226, 2006.

Donat, M. G., Alexander, L. V., Yang, H., Durre, I., Vose, R., Dunn, R. J. H., Willett, K. M., Aguilar, E., Brunet, M., Caesar, J., Hewitson, B., Jack, C., Tank, A. M. G. K., Kruger, A. C., Marengo, J., Peterson, T. C., Renom, M., Rojas, C. O., Rusticucci, M., Salinger, J., Elrayah, A. S., Sekele, S. S., Srivastava, A. K., Trewin, B., Villarroel, C., Vincent, L. A., Zhai, P., Zhang, X., and Kitching, S.: Updated analyses of temperature and precipitation extreme indices since the beginning of the twentieth century: The HadEX2 dataset, Journal of Geophysical Research: Atmospheres, 118, 2098-2118, 2013.

Doocy, S., Daniels, A., Murray, S., and Kirsch, T.: The Human impact of floods: a historical review of events 1980-2009 and systematic literature review, PLoS Curr, Disasters, 5, 2013.

EPA, U.: Storm Water Management Model, 2016. 2016.

Feyen, L., Barredo, J., and Dankers, R.: Implications of global warming and urban land use change on flooding in Europe, Water & Urban Development Paradigms-Towards an integration of engineering, design and management approaches, 2009. 217-225, 2009.

Fowler, H. J., Blenkinsop, S., and Tebaldi, C.: Linking climate change modelling to impacts studies: recent advances in downscaling techniques for hydrological modelling, International Journal of Climatology, 27, 1547-1578, 2007.

Franz, K. J. and Hogue, T. S.: Evaluating uncertainty estimates in hydrologic models: borrowing measures from the forecast verification community, Hydrology and Earth System Sciences, 15, 3367-3382, 2011.

Füssel, H. M.: Adaptation planning for climate change: concepts, assessment approaches, and key lessons, Sustainability Science, 2, 265-275, 2007.

García-Bartual, R. and Andrés-Doménech, I.: A two parameter design storm for Mediterranean convective rainfall, Hydrology and Earth System Sciences Discussions, doi: 10.5194/hess-2016-644, 2016. 1-19, 2016.

Geert, L. and Jisk, A.: A simple scaling approach to produce climate scenarios of local precipitation extremes for the Netherlands, Environmental Research Letters, 10, 085001, 2015.

Graham, L. P., Andréasson, J., and Carlsson, B.: Assessing climate change impacts on hydrology from an ensemble of regional climate models, model scales and linking methods – a case study on the Lule River basin, Climatic Change, 81, 293-307, 2007.

Gui-shan, Y.: Historical change and future trends of storm surge disaster in China's coastal area [J], Journal of Natural Disasters, 3, 003, 2000.

Hardwick Jones, R., Westra, S., and Sharma, A.: Observed relationships between extreme sub-daily precipitation, surface temperature, and relative humidity, Geophysical Research Letters, 37, 2010.

Hartmann, D. L., Klein Tank, A. M., Rusticucci, M., Alexander, L. V., Brönnimann, S., Charabi, Y. A. R., Dentener, F. J., Dlugokencky, E. J., Easterling, D. R., and Kaplan, A.: Climate Change 2013 the Physical Science Basis: Working Group I Contribution to the Fifth Assessment Report of the Intergovernmental Panel on Climate Change, 2013.

Hettiarachchi, S. L., Johnson M. J. http://www.swwdmn.org/pdf/projects/completed/2006%20Stormwater%20Modeling%20Report_HDR.pdf, 2006

Hettiarachchi. S, Beduhn. R, Christopherson. J Moore. M, Managing Surface Water for Flood Damage Reduction, World Water and Environmental Resources Congress 2005, | Anchorage, Alaska, United States, doi-10.1061/40792(173)321 May 15-19, 2005

Hogg, W.: Time distribution of short duration storm rainfall in Canada, 1980, 56-63.

Huff, F. A.: Time distribution of rainfall in heavy storms, Water Resources Research, 3, 1007-1019, 1967.

IPCC, 2014: Climate Change 2014: Synthesis Report. Contribution of Working Groups I, II and III to the Fifth Assessment Report of the Intergovernmental Panel on Climate Change [Core Writing Team, R.K. Pachauri and L.A. Meyer (eds.)]. IPCC, Geneva, Switzerland, 151 pp.

Jones, P., Trenberth, K., Ambenje, P., Bojariu, R., Easterling, D., Klein, T., Parker, D., Renwick, J., Rusticucci, M., and Soden, B.: Observations: surface and atmospheric climate change, Climate change 2007: the physical science basis. Contribution of Working Group I to the Fourth Assessment Report of the Intergovernmental Panel on Climate Change, 2007. 235-336, 2007.

Kay, A. L., Davies, H. N., Bell, V. A., and Jones, R. G.: Comparison of uncertainty sources

for climate change impacts: flood frequency in England, Climatic Change, 92, 41-63, 2009.

Kharin, V. V., F. W. Zwiers, X. Zhang, and M. Wehner (2013), Changes in temperature and precipitation extremes in the CMIP5 ensemble, Clim. Change, 119(2), 345–357, doi:10.1007/s10584-013-0705-8.

Lambourne, J. J. and Stephenson, D.: Model study of the effect of temporal storm distributions on peak discharges and volumes, Hydrological Sciences Journal, 32, 215-226, 1987.

Leander, R., Buishand, T. A., van den Hurk, B. J. J. M., and de Wit, M. J. M.: Estimated changes in flood quantiles of the river Meuse from resampling of regional climate model output, Journal of Hydrology, 351, 331-343, 2008.

Lenderink, G. and Attema, J.: A simple scaling approach to produce climate scenarios of local precipitation extremes for the Netherlands, Environmental Research Letters, 10, 085001, 2015.

Lenderink, G., Mok, H., Lee, T., and Van Oldenborgh, G.: Scaling and trends of hourly precipitation extremes in two different climate zones–Hong Kong and the Netherlands, Hydrology and Earth System Sciences, 15, 3033-3041, 2011.

Lenderink, G. and van Meijgaard, E.: Increase in hourly precipitation extremes beyond expectations from temperature changes, Nature Geoscience, 1, 511-514, 2008.

Mamo, T. G.: Evaluation of the Potential Impact of Rainfall Intensity Variation due to Climate Change on Existing Drainage Infrastructure, Journal of Irrigation and Drainage Engineering, 141, 05015002, 2015.

Manola, I., van den Hurk, B., De Moel, H., and Aerts, J.: Future extreme precipitation intensities based on historic events, Hydrol. Earth Syst. Sci. Discuss., https://doi.org/10.5194/hess-2017-227, in review, 2017.

Maraun, D., Wetterhall, F., Ireson, A. M., Chandler, R. E., Kendon, E. J., Widmann, M., Brienen, S., Rust, H. W., Sauter, T., Themeßl, M., Venema, V. K. C., Chun, K. P., Goodess, C. M., Jones, R. G., Onof, C., Vrac, M., and Thiele-Eich, I.: Precipitation downscaling under climate change: Recent developments to bridge the gap between dynamical models and the end user, Reviews of Geophysics, 48, 2010.

Meehl, G. A., Stocker, T. F., Collins, W. D., Friedlingstein, A., Gaye, A. T., Gregory, J. M., Kitoh, A., Knutti, R., Murphy, J. M., and Noda, A.: Global climate projections, 2007. 2007.

Merz, B., Kreibich, H., Schwarze, R., and Thieken, A.: Review article" Assessment of economic flood damage", Natural Hazards and Earth System Sciences, 10, 1697, 2010.

Milly, P., Julio, B., Malin, F., Robert, M., Zbigniew, W., Dennis, P., and Ronald, J.: Stationarity is dead, Ground Water News & Views, 4, 6-8, 2007.

Mishra, V., Wallace, J. M., and Lettenmaier, D. P.: Relationship between hourly extreme

precipitation and local air temperature in the United States, Geophysical Research Letters, 39, 2012.

Molnar, P., Fatichi, S., Gaál, L., Szolgay, J., and Burlando, P.: Storm type effects on super Clausius–Clapeyron scaling of intense rainstorm properties with air temperature, Hydrol. Earth Syst. Sci, 19, 1753-1766, 2015.

Nandakumar, N. and Mein, R. G.: Uncertainty in rainfall—runoff model simulations and the implications for predicting the hydrologic effects of land-use change, Journal of Hydrology, 192, 211-232, 1997.

Nguyen, V. T., Desramaut, N., and Nguyen, T. D.: Optimal rainfall temporal patterns for urban drainage design in the context of climate change, Water Sci Technol, 62, 1170-1176, 2010.

Packman, J. and Kidd, C.: A logical approach to the design storm concept, Water Resources Research, 16, 994-1000, 1980.

Panthou, G., Mailhot, A., Laurence, E., and Talbot, G.: Relationship between surface temperature and extreme rainfalls: A multi-time-scale and event-based analysis, Journal of Hydrometeorology, 15, 1999-2011, 2014.

Perica, S., D. Martin, S. Pavlovic, I. Roy, M. St. Laurent, C. Trypaluk, D. Unruh, M. Yekta, and G. Bonnin NOAA Atlas 14 precipitation- frequency Atlas of the United States Volume 9 Version 2.0: Southeastern States (Alabama, Arkansas, Florida, Georgia, Louisiana, Mississippi), 2013. 2013.

Peters, G. P., Andrew, R. M., Boden, T., Canadell, J. G., Ciais, P., Le Quéré, C., Marland, G., Raupach, M. R., and Wilson, C.: The challenge to keep global warming below 2? C, Nature Climate Change, 3, 4, 2013.

Pilgrim, D.: Section 1 - Flood routing, in Australian Rainfall and Runoff - A Guide to Flood Estimation, 1997. 1997.

Prudhomme, C. and Davies, H.: Assessing uncertainties in climate change impact analyses on the river flow regimes in the UK. Part 2: future climate, Climatic Change, 93, 197-222, 2009.

Prudhomme, C., Reynard, N., and Crooks, S.: Downscaling of global climate models for flood frequency analysis: where are we now?, Hydrological processes, 16, 1137-1150, 2002.
Quan, V. M. W. H. M. H. M. D. E. W. C. C. H. Q. D.: National Engineering Handbook Chapter 4- Storm Rainfall Depth and Distribution, 2015. 2015.

Raff, D., Pruitt, T., and Brekke, L.: A framework for assessing flood frequency based on climate projection information, Hydrology and Earth System Sciences, 13, 2119, 2009.

Renard, B., Kavetski, D., Kuczera, G., Thyer, M., and Franks, S. W.: Understanding predictive uncertainty in hydrologic modeling: The challenge of identifying input and structural errors, Water Resources Research, 46, 2010.

Rivard, G.: Design Storm Events for Urban Drainage Based on Historical Rainfall Data:A

Conceptual Framework for a Logical Approach, Journal of Water Management Modeling, Rl91-12, 187-199, 1996.

Sandink, D.: Urban flooding and ground-related homes in Canada: an overview, Journal of Flood Risk Management, 2015. 2015.

Schreider, S. Y., Smith, D. I., and Jakeman, A. J.: Climate Change Impacts on Urban Flooding, Climatic Change, 47, 91-115, 2000.

Seneviratne, S. I., Nicholls, N., Easterling, D., Goodess, C. M., Kanae, S., Kossin, J., Luo, Y., Marengo, J., McInnes, K., and Rahimi, M.: Changes in climate extremes and their impacts on the natural physical environment, Managing the risks of extreme events and disasters to advance climate change adaptation, 2012. 109-230, 2012.

Sillmann, J., Kharin, V., Zwiers, F., Zhang, X., and Bronaugh, D.: Climate extremes indices in the CMIP5 multimodel ensemble: Part 2. Future climate projections, Journal of Geophysical Research: Atmospheres, 118, 2473-2493, 2013.

Singh, V. P. and Woolhiser, D. A.: Mathematical modeling of watershed hydrology, Journal of hydrologic engineering, 7, 270-292, 2002.

Smith, B. K., Smith, J., and Baeck, M. L.: Flash Flood–Producing Storm Properties in a Small Urban Watershed, Journal of Hydrometeorology, 17, 2631-2647, 2016.

Smith, B. K., Smith, J., and Baeck, M. L.: Flash Flood–Producing Storm Properties in a Small Urban Watershed, Journal of Hydrometeorology, 17, 2631-2647, 2016.

Sørup, H. J. D., Christensen, O. B., Arnbjerg-Nielsen, K., and Mikkelsen, P. S.: Downscaling future precipitation extremes to urban hydrology scales using a spatio-temporal Neyman–Scott weather generator, Hydrology and Earth System Sciences, 20, 1387-1403, 2016.

Šraj, M., Dirnbek, L., and Brilly, M.: The influence of effective rainfall on modeled runoff hydrograph, Journal of Hydrology and Hydromechanics, 58, 2010.

Trenberth, K. E.: Changes in precipitation with climate change, Climate Research, 47, 123-138, 2011.

United Nations, D. o. E. a. S. A., Population Division: World Urbanization Prospects: The 2014 Revision, Highlight, 2014. 2014.

van Pelt, S. C., Kabat, P., ter Maat, H. W., van den Hurk, B. J. J. M., and Weerts, A. H.: Discharge simulations performed with a hydrological model using bias corrected regional climate model input, Hydrol. Earth Syst. Sci., 13, 2387-2397, 2009.

Vrugt, J. A., Braak, C. J. F. t., Clark, M. P., Hyman, J. M., and Robinson, B. A.: Treatment of input uncertainty in hydrologic modeling: Doing hydrology backward with Markov chain Monte Carlo simulation, Water Resources Research, 44, 2008.

Wasko, C., Parinussa, R., and Sharma, A.: A quasi-global assessment of changes in remotely sensed rainfall extremes with temperature, Geophysical Research Letters, 2016. 2016.

Wasko, C. and Sharma, A.: Continuous rainfall generation for a warmer climate using observed temperature sensitivities, Journal of Hydrology, 544, 575-590, 2017.

Wasko, C. and Sharma, A.: Quantile regression for investigating scaling of extreme precipitation with temperature, Water Resources Research, 50, 3608-3614, 2014.

Wasko, C. and Sharma, A.: Steeper temporal distribution of rain intensity at higher temperatures within Australian storms, Nature Geosci, 8, 527-529, 2015.

Wasko, C., Sharma, A., and Johnson, F.: Does storm duration modulate the extreme precipitation-temperature scaling relationship?, Geophysical Research Letters, 42, 8783-8790, 2015.

Wasko, C., Sharma, A., and Westra, S.: Reduced spatial extent of extreme storms at higher temperatures, Geophysical Research Letters, 43, 4026-4032, 2016.

Westra, S., Alexander, L. V., and Zwiers, F. W.: Global Increasing Trends in Annual Maximum Daily Precipitation, Journal of Climate, 26, 3904-3918, 2013.

Westra, S., Evans, J. P., Mehrotra, R., and Sharma, A.: A conditional disaggregation algorithm for generating fine time-scale rainfall data in a warmer climate, Journal of Hydrology, 479, 86-99, 2013.

Wilks, D. S.: Use of stochastic weathergenerators for precipitation downscaling, Wiley Interdisciplinary Reviews: Climate Change, 1, 898-907, 2010.

Willems, P., Arnbjerg-Nielsen, K., Olsson, J., and Nguyen, V. T. V.: Climate change impact assessment on urban rainfall extremes and urban drainage: Methods and shortcomings, Atmospheric Research, 103, 106-118, 2012.

Woldemeskel, F. M., Sharma, A., Mehrotra, R., and Westra, S.: Constraining continuous rainfall simulations for derived design flood estimation, Journal of Hydrology, 542, 581-588, 2016.

Wood, E. F.: An analysis of the effects of parameter uncertainty in deterministic hydrologic models, Water Resources Research, 12, 925-932, 1976.

Wood, E. F. and Rodríguez-Iturbe, I.: Bayesian inference and decision making for extreme hydrologic events, Water Resources Research, 11, 533-542, 1975.

Woolhiser, V. P. S. a. D. A.: mathematical modelling of watershed hydology, JOURNAL OF HYDROLOGIC ENGINEERING, 7, 270-292, 2002.

Zheng, Y. and Keller, A. A.: Uncertainty assessment in watershed-scale water quality modeling and management: 1. Framework and application of generalized likelihood uncertainty estimation (GLUE) approach, Water Resources Research, 43, 2007.

950 Zhou, Q., Leng, G., and Huang, M.: Impacts of future climate change on urban flood risks:
951 benefits of climate mitigation and adaptations, Hydrology and Earth System Sciences
952 Discussions, doi: 10.5194/hess-2016-369, 2016. 1-31, 2016.
953
954 Zhou, X., Bai, Z., and Yang, Y.: Linking trends in urban extreme rainfall to urban flooding in
955 China, International Journal of Climatology, doi: 10.1002/joc.5107, 2017. 2017.
956
957 Zope, P. E., Eldho, T. I., and Jothiprakash, V.: Impacts of land use–land cover change and
958 urbanization on flooding: A case study of Oshiwara River Basin in Mumbai, India,
959 CATENA, 145, 142-154, 2016.
960